

# Retrofitting Biomass Combined Heat and Power Plant for Biofuel Production

Hao Chen <sup>a,\*</sup>, Daheem Mehmood <sup>a</sup>, Erik Dahlquist <sup>a</sup>, Konstantinos Kyprianidis <sup>a</sup>

<sup>a</sup> School of Business, Society and Engineering, Mälardalen University, PO Box 883, SE-721 23 Västerås, Sweden  
hao.chen@mdu.se

## Abstract

Thermochemical conversion processes of biomass, such as gasification and pyrolysis, can convert a wide range of feedstocks into liquid fuels, including forest residue, agricultural, food, and municipal solid waste. These more widely available and theoretically lower cost feedstocks make biofuel production through thermochemical pathway more cost-competitive. Furthermore, the thermochemical conversion pathway for biomass conversion could be relatively easy to integrate with the existing biomass combined heat and power plant, making it an attractive technology for the future commercialization of biofuel production through biomass. A detailed analysis was undertaken of a retrofitted biomass combined heat and power plant for biofuel production in this work. The biofuel production plant is designed to explore the polygeneration of hydrogen, biomethane, and bio-oil via the integration of gasification, pyrolysis, and renewable-powered electrolysis. The G-valve in the biomass circulating fluid bed plant, which is generally used for sand and char recycling, is retrofitted in the proposed system to fit the pyrolysis reaction for bio-oil production. Centering around the biomass circulating fluid bed gasifier, the system is also outfitted with a condensation and distillation process for bio-oil production, and a membrane reactor system for biomethane production. A mathematical model of the proposed biofuel production plant is established in Aspen Plus, followed by a performance investigation of the biofuel production plant under various design conditions. The limitations and opportunities of this retrofitted biomass combined heat and power plant for biofuel production are explored in this study.

## 1. Introduction

Biomass has been acknowledged as a premier renewable energy resource in the EU. Among various biomass conversion pathways, thermochemical conversion processes such as gasification and pyrolysis, are capable of producing biofuels from a diverse of feedstocks, including forest residuals, agricultural waste products, food waste, and municipal solid waste. These theoretically low-cost feedstocks make the thermochemical pathways of biomass conversion more economically viable for biofuels production [1].

As a thermochemical pathway for biomass conversion, fast pyrolysis has the potential to be integrated into existing biomass combined heat and power (CHP) plants [2], thereby enhancing its cost competitiveness for biofuel production. Karvonen et al. performed an environmental assessment on the integration of fast pyrolysis into a CHP plant [3]. This integration was achieved by using the heat from the char and non-condensing gas combustion to enhance heat and power generation in a CHP plant. The results indicated that the efficiency of stand-alone pyrolysis was improved from 59% to

71% upon integration into a CHP plant. A study on the integration of biomass fast pyrolysis with a municipal waste CHP plant was conducted by Kohl et al. [4]. The heat required in the biomass pyrolysis process was supplied by the hot flue gas from the CHP plant in this work, aiming at improving the pyrolysis product yield and retaining the district heat load simultaneously. It is noted that the operational hours of the CHP plant could be potentially increased by 57%, which makes this integration economically viable. Onarheim et al. performed a techno-economic analysis of a fast pyrolysis bio-oil production process with integration into an existing Fluid Bed Boiler CHP plant [5]. The sand heated in the CHP plant was sent to support the endothermic reaction in the pyrolysis reactor. Sensitivity analysis on different feedstocks and varying heat and electricity prices were also implemented in this study. The results showed that the economically advantages of this integration highly depend on the cost of heat and feedstocks. Zetterholm et al. completed a comprehensive evaluation of fast pyrolysis value chain configurations considering different types of locations, emissions, feedstocks, and final products [6]. The results showed that production cost for

crude pyrolysis liquid is in the range of 36-60 €/MWh (LHV of pyrolysis crude oil), and 61-90 €/MWh after further upgrading pyrolysis crude oil to diesel and petrol. It was also found that the integration of existing industrial infrastructure helps to mitigate the production cost.

Various gasification technologies are also considered in biofuel production processes since they provide excellent synergies. As a thermochemical process, biomass gasification can benefit from the integration of existing CHP plants. Piazzi et al. performed an experimental study to investigate the feasibility of retrofitting existing small-scale gasifier from CHP production to hydrogen and biofuel generation [7]. Co-production of syngas and biofuel by using the dual fluidized bed gasifier has been examined by Gustavsson et al., demonstrated a substantial enhancement on system efficiency [8]. An economic feasibility analysis of complementing existing CHP plants for hydrogen production was investigated by Naqvi et al., in this research the estimation cost for hydrogen production is 0.125-0.75 €/kg hydrogen [9]. Thunman et al. conducted an economic analysis of the GoBiGas plant, which is the first industrial installation for biomethane production with gasification [10]. This study found that the economic performance could be improved if integrated with existing infrastructure and low-grade feedstocks. Holmgren et al. examined the performance of gasification-based biofuel production systems with integration of district heating system [11]. It is concluded that the profitability of this system strongly depends on the specific production technologies and on the reference power production. The integration of existing CHP plant and gasification process for dimethyl ether or methanol production was analyzed by Salman et al. [12]. The results showed that the profitability could be notably improved by integrating gasification with CHP plants for biofuel production, as compared with the CHP plants that are only for heat and electricity generation.

In this study, a detailed analysis was undertaken of a retrofitted biomass combined heat and power plant for biofuel production. By retrofitting the G-valve in the biomass circulating fluid bed boiler for pyrolysis, the biofuel production process can benefit from the heat and hydrogen generation from the biomass gasification. It is expected that the proposed system could reduce the investment cost of biofuel production, and the integrated technologies could also serve as a solution for energy storage and transportation for renewables integration.

## 2. System description

The proposed pilot plant is designed to explore the polygeneration of hydrogen, biomethane, and bio-oil via the integration of biomass gasification, pyrolysis, and electrolysis with utilizing renewable energy. The primary component of the pilot plant is a Circulating Fluidized Boiler (CFB) with biomass as feedstock. The G-valve, typically used for sand and char recycling in the CFB, is retrofitted to fit the biomass pyrolysis reaction for biooil production. Centering around the Biomass CFB, the plant is also outfitted with cooling and distillation for bio-oil production, and membrane reactor system for biomethane production.

The schematic diagram of the facility is presented in Figure 1. During operation, ambient air is preheated to around 600 °C before being fed into the CFB, where the air transports and heats the feeding biomass up to enable the gasification process to occur downstream.

Then syngas generated from biomass gasification is separated from the solids (uncombusted biomass, char, and sand) in the cyclone. The solids, which still carry heat, are directed to the G-Valve (pyrolyzer), where the sensible heat of the solids is used to support the endothermic pyrolysis reaction and to generate pyrolysis vapor. After the cooling process within a condenser, the pyrolysis vapor becomes liquid bio-oil, which will be further upgraded to bio-gasoline or biodiesel in the hydrotreatment reactors with the presence of hydrogen. Meanwhile, the syngas after the cyclone will go through a reformer and a two-stage water-gas shift reactor to enhance the hydrogen generation. Finally, the existing carbon monoxide and carbon dioxide in the syngas, together with the generated hydrogen, is sent to a methanation reactor for biomethane generation.

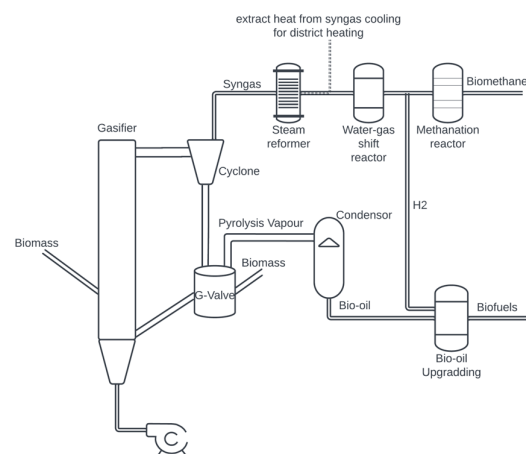


Figure 1, Schematic diagram of biomass pyrolysis, gasification, and electrolysis integrated polygeneration system

### 3. Process modeling

#### 3.1 Biomass pyrolysis integrated with gasification

The process model for the entire biofuel production pilot plant was established in Aspen Plus to evaluate the system performance. Figure 2 illustrates the flowsheet of incorporating the pyrolysis process into the biomass CFB gasifier in Aspen Plus. The gasification was simulated by using two blocks, namely the DECOM block (RYield reactor) and the Gasifier block (Gibbs Reactor). Biomass is first converted into conventional components (C, H<sub>2</sub>, O<sub>2</sub>, N<sub>2</sub>, S and ash) in the DECOM block, in which the product yield is calculated by an external Fortran code based on mass balance. The Gasifier block mixes the products from DECOM with air and simulates the gasification process by computing thermodynamic equilibrium.

A RYield reactor (Pyrolyzer block in Figure 2) is also used to conduct the pyrolysis process in the G-Valve. The mass yield fraction of pyrolysis product was taken from Lisa et al. [13] with the fixed pyrolysis temperature at 480 °C. Char and ash generated from pyrolysis, along with recycled sand, are then directed to the Char Combustor block, where the solid char will be combusted. If needed, additional air will also be injected to the Biomass Comb block to supply heat for the pyrolysis. Part of the preheated air is also injected into the gasifier to support the endothermic gasification reaction. SiO<sub>2</sub> is used in this study to simulate sand in the Gasifier. The normalized feedstock ultimate analysis and the product yield for the pyrolysis reactor are given in Table 1. Peng Robinson cubic equation of state with the Boston-Mathias alpha function is used in Aspen Plus for all thermodynamic properties.

Table 1, Ultimate analysis of the feedstock and product yield for the pyrolysis

Ultimate analysis of the feedstock		Product yield for the pyrolysis	
Carbon	49.66 %	H <sub>2</sub>	0.0000
Hydrogen	6.31 %	CO	0.0582
Oxygen	43.55 %	CO <sub>2</sub>	0.0603
Nitrogen	0.10 %	CH <sub>4</sub>	0.0028
Sulfur	0.08 %	C <sub>2</sub> H <sub>4</sub>	0.0028
Ash	0.30 %	Acetic Acid,	0.1107
		C <sub>2</sub> H <sub>4</sub> O <sub>2</sub>	
LHV	15.1 MJ/kg	Acetone,	0.1272
		C <sub>3</sub> H <sub>6</sub> O	
		M-Cresol,	0.0398
		C <sub>7</sub> H <sub>8</sub> O	
		Coniferyl	0.0068
		Aldehyde,	
		C <sub>10</sub> H <sub>10</sub> O <sub>3</sub>	

Guaiacol,	0.2680
C <sub>7</sub> H <sub>8</sub> O <sub>2</sub>	
Levogluconan,	0.0440
C <sub>6</sub> H <sub>10</sub> O <sub>5</sub>	
Furfural,	0.0294
C <sub>5</sub> H <sub>4</sub> O <sub>2</sub>	
Water, H <sub>2</sub> O	0.1480
Char	0.0968

#### 3.2 Bio-oil production and upgrading with onsite hydrogen generation

The pyrolysis vapor generated from the G-valve (Pyrolyzer) needs to be condensed to form bio-oil. To achieve this, a quench loop, depicted in Figure 3, is implemented to facilitate the condensation of the pyrolysis vapor into a liquid phase. The pyrolysis gas after the quench loop is sent back to the Char Combustion block (shown in Figure 2) to support the heat for gasification.

After the quench loop, bio-oil is separated from the aqueous phases in the pyrolysis product. To enhance the stability and heating value of the bio-oil, a hydrotreatment process is employed after the quench loop. The hydrotreatment reactions and operating parameters employed in the Hydrotreatment Reactor block are taken from Dutta et al. [14]. The product resulting from the hydrotreatment process is directed to the distillation column, where biofuel is separated out and produced. It is worth mentioning that the hydrogen required for the bio-oil upgrading is from gasification, which enables onsite self-sufficient hydrogen generation.

#### 3.3 Bio-methane generation with renewables integration

As presented in Figure 4, to enhance the biofuel production of the pilot plant, syngas produced from the gasification process is mixed with the recycled gas from the bio-oil upgrading process and directed to the steam reformer to increase hydrogen production. To further increase hydrogen generation, a two-stage water-gas shift reactor (high temperature water-gas shift reactor, HT-WGS, and low temperature water-gas shift reactor, LT-WGS) is incorporated after the reformer. Subsequently, in the pressure swing adsorption (PSA) process, a portion of the hydrogen is diverted to the bio-oil upgrading process, while the remaining gas (primarily composed of H<sub>2</sub>, CO, and CO<sub>2</sub>) is compressed and channeled to the methanation reactor to produce bio-methane, aiming for enhanced biofuel production and carbon capture and utilization. Additionally, air preheating and high temperature steam generation are implemented into the process to improve the thermal efficiency of the entire pilot plant.

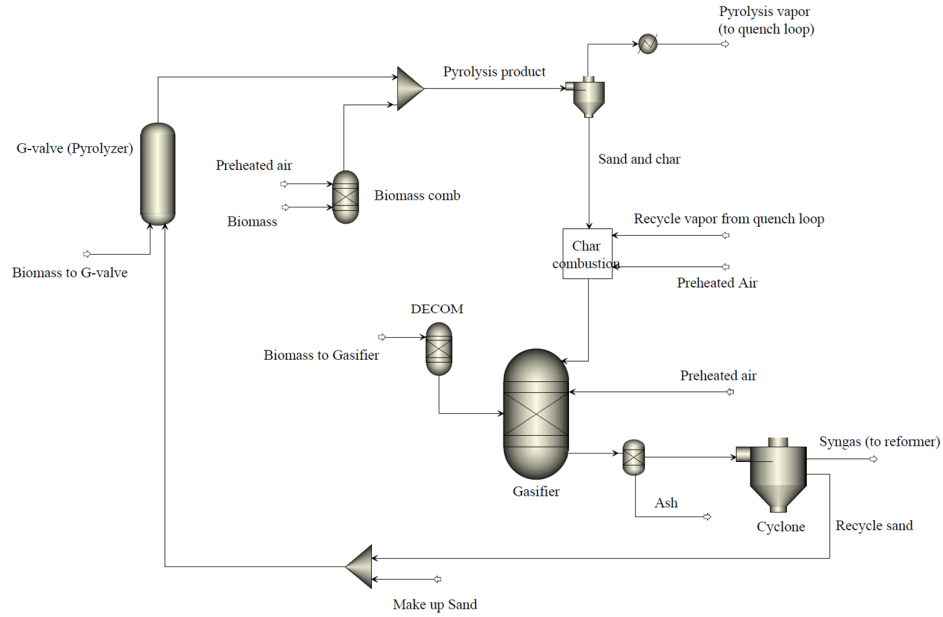


Figure 2, Process flowsheet of biomass pyrolysis integrated with gasification process in Aspen Plus

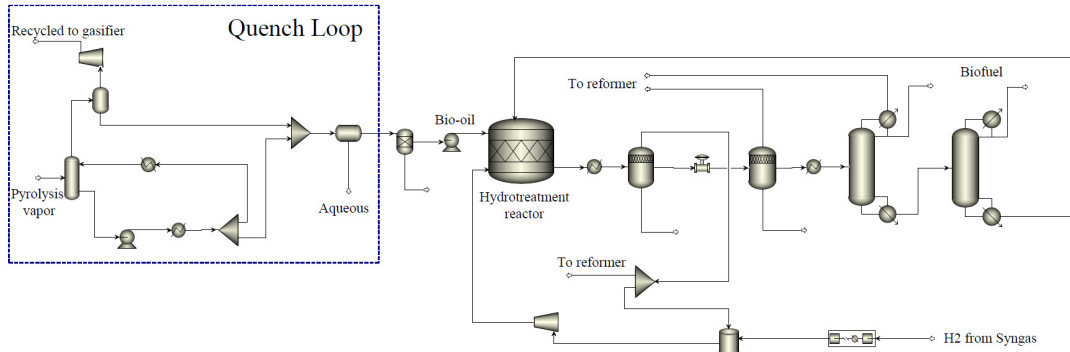


Figure 3, Process flowsheet of Bio-oil production and upgrading process in Aspen Plus

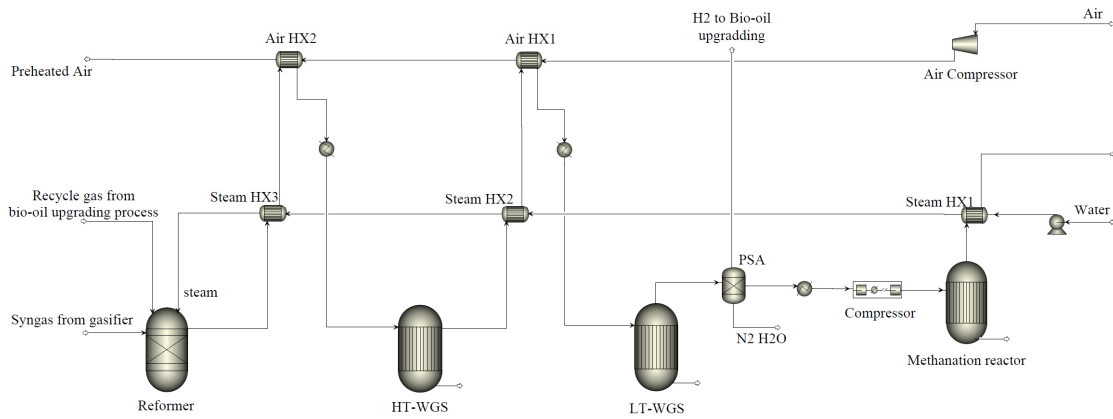


Figure 4, Process flowsheet of hydrogen and biomethane production process in Aspen Plus

## 4. Results

### 4.1 process modeling results

The goal of the process modeling is to determine the optimal parameters for the plant design to improve fuel production and profitability. In this baseline scenario, electrolyzers are not integrated in the polygeneration system. Based on the capacity of the pilot plant that is under construction at Malardalen University, the biomass feeding into the gasifier and pyrolyzer (G-Valve) are fixed at 45kg/hr and 15 kg/hr respectively,

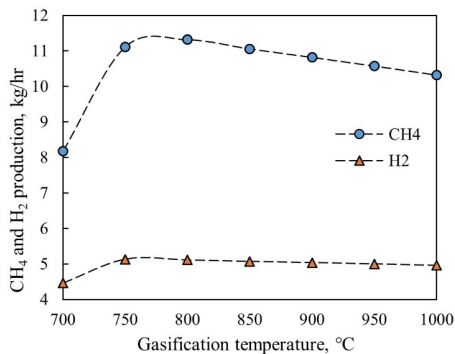


Figure 5, CH<sub>4</sub> production after the methanation reactor and H<sub>2</sub> production after LT-WGS reactor

As aforementioned, the pyrolysis and gasification process are coupled in the polygeneration plant by taking the heat from the recycling sand to support the endothermic pyrolysis process. The uncombusted solid left from the pyrolysis is then recycled back to the gasifier to participate in the gasification process. Therefore, the operating condition of the gasifier has a major impact on the downstream processes such as bio-oil production, hydrogen and biomethane generation. A sensitivity analysis is performed in this work to investigate the impacts of operating temperature of gasifier on hydrogen and methane production of the proposed system. Figure 5 shows the methane production (after methanation reactor) and hydrogen yield (after the LT-WGS reactor) when the gasification temperature varies from 700 to 1000 °C. As illustrated in Figure 5, CH<sub>4</sub> and H<sub>2</sub> production increase when gasification temperature rises from 700 to 800 °C, after which the CH<sub>4</sub> and H<sub>2</sub> yields start to drop if further increasing the gasification temperature from 800 to 1000 °C. The reason behind the peak production of H<sub>2</sub> and CH<sub>4</sub> at 800 °C gasification temperature is that, while gasification benefits from the higher temperature, more air is required to support the higher gasification temperature through combustion, thus resulting in the reduced CO, H<sub>2</sub>, and CH<sub>4</sub> in the syngas composition, and eventually causing the

drop of H<sub>2</sub> and CH<sub>4</sub> production after WGS reactor and methanation reactor.

Figure 6 shows the gas composition change along with the process streams (after gasification, reforming, and two stage water-gas shift reaction), it can be seen that hydrogen composition in the syngas increased significantly after reforming and water-gas shift reaction.

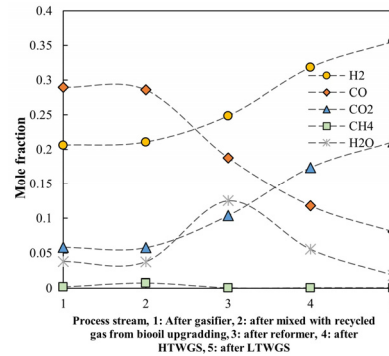


Figure 6, Mole concentration at varied location of the process line

### 4.2 Air, heat, and power consumption

Air and power consumption of the polygeneration system under varied operating gasification temperatures are summarized in Figure 7. As we discussed before, more air is injected into the gasifier to maintain a higher gasification temperature, which contributes to the increase in air consumption. As also shown in Figure 7a, in the case of gasification temperature lower than 800 °C, the heat carried by the recycled sand is not enough to support the endothermic reaction, therefore air is feeding into the pyrolyzer to support the pyrolysis process. The same happens in the steam reformer reactor, air is also injected into the reformer to supply the heat (so called auto-thermal reforming). It is worth noting that the air required by the pyrolysis and reformer are calculated and controlled by an external Fortran code integrated in Aspen Plus.

Figure 7b demonstrates the power consumption of the polygeneration plant under different operating conditions. As shown in Figure 7b, more than half of the power consumption comes from the gas compression for the methanation. The methanation reactor operates at a high pressure above 30 bars, which consumes a large amount of power (about 20 kW, shown in Figure 7b) to pressurize the syngas before feeding into the methanation reactor. The second largest power consumption in the system is from the hydrogen compressor, as shown in Figure 7b. Hydrogen compressor is employed to compress the hydrogen (generated from the gasification, reforming, and water-gas shifting process) to the operating pressure (40 bar) of the bio-oil

hydrotreatment reactor, therefore resulting in an unneglectable proportion of power consumption.

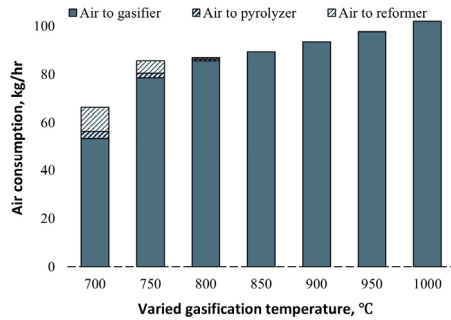


Figure 7a, Air consumption in the polygeneration system

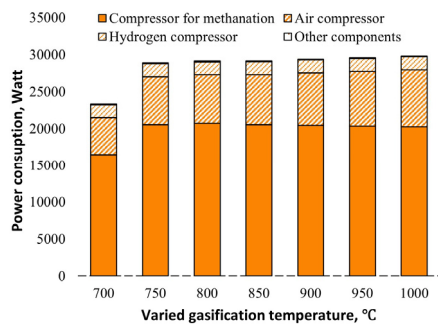


Figure 7b, Power consumption in the polygeneration system, baseline scenario

Heat requirements and the heat produced in the polygeneration plant are described in Figure 8. The heat demand comes mainly from the bio-oil upgrading process, such as hydrotreatment process, water separation and distillation process, about 2.8 kW. The operating conditions of the gasifier hardly affect the bio-oil production process, thus resulting in the nearly constant heat requirement with varied gasification temperatures, as shown in Figure 8a. Figure 8b shows the changes of the heat produced in the polygeneration plant, as more combustion is required to support the higher gasification temperature, more heat released from the system, around 9 - 10 kW, which provides an opportunity to be used for district heating.

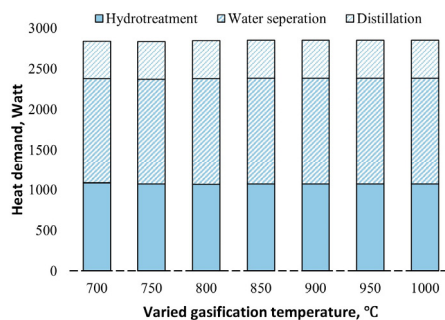


Figure 8a, Heat demand in the polygeneration system

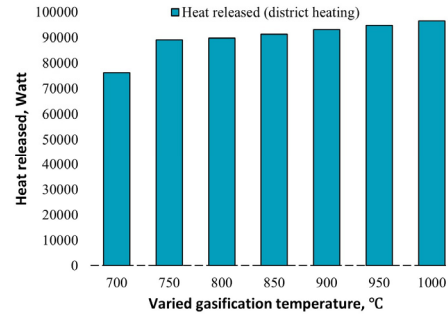


Figure 8b, Heat produced in the polygeneration system

### 4.3 Carbon efficiency

Figure 9 shows the carbon distribution and carbon efficiency of the polygeneration system under varied gasification temperatures. Carbon efficiency represents the proportion of carbon that has been converted into biofuels from the feedstock. As shown in Figure 9, around 40% of the carbon from the biomass could be captured in biomethane and bio-oil. The optimal gasification temperature in terms of the highest carbon efficiency (around 40%) is 800 °C. And it is also worth noting that a large proportion of carbon is left in the ash when the operating temperature of gasifier is lower than 750 °C, which is not favorable.

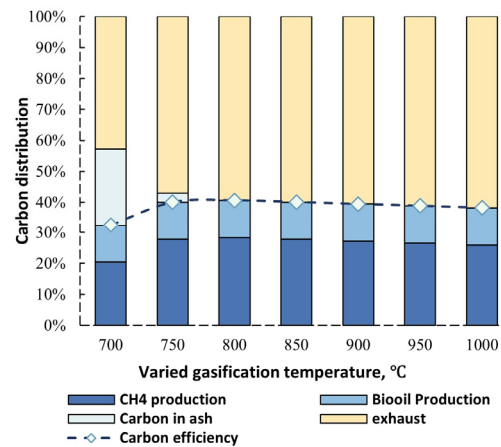


Figure 9, Carbon distribution in the final products and carbon efficiency of the polygeneration system

Figure 10 illustrates the carbon flows in the polygeneration system in the case of 800 °C gasification temperature. It is obvious that more than half of the carbon is still released into the atmosphere through waste and exhaust in this case.

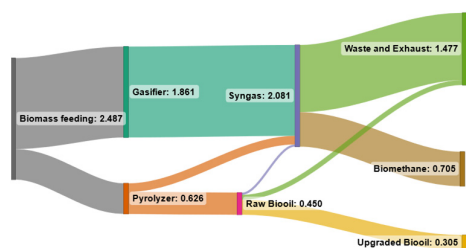


Figure 10, Carbon flows (kmol/hr) in the polygeneration system with 800 °C gasification temperature

Since the capacity of the pyrolyzer (G-Valve) could be relatively easy to scale up, a sensitivity analysis of pyrolyzer capacity (varied biomass feeding mass flowrate from 15 kg/hr to 45 kg/hr) is performed in this work. Table 2 summarizes the fuel productions and carbon efficiencies of the polygeneration system under varied pyrolyzer capacities, while the gasifier operating temperature and the biomass feeding flowrate in the gasifier are fixed at 800 °C and 45 kg/hr respectively in this case.

Table 2, Fuel productions and carbon efficiencies of the polygeneration system

Biomass to pyrolyzer (kg/hr)	Biooil production (kg/hr)	Lower heating value of biomethane (kWh/kg)	Biomethane production (kg/hr)	Carbon efficiency (%)
15	4.8	10.1	11.3	40.6
30	9.5	10.1	12.5	43.9
45	14.2	10.1	13.5	45.7

## 5. Summary and Discussions

A polygeneration system of retrofitting the existing biomass CHP plant for biofuel production was proposed and analyzed in this work. The process modeling of the polygeneration system, which integrates biomass gasification and pyrolysis to generate biofuels (biooil and biomethane), is performed in Aspen Plus. Sensitivity analysis of the key design parameters, such as gasification temperature, was conducted to investigate the impacts on system performance.

Retrofitting of existing CHP plant for biofuel production provides good opportunities for sustainable fuel generation and surplus renewable energy storage. By the integration of gasification and pyrolysis, the uncombusted char left from pyrolysis could be used to support the endothermic gasification process, and the hydrogen generated from gasification could be used to upgrade the biooil through hydrotreatment, thus improving the fuel production and profitability of such systems. The results also shows that the optimal gasification temperature in terms of enhancing biomethane and hydrogen production is 800 °C. The carbon

efficiency of the entire system could reach up to 40%.

It can be expected that when integrated with renewable energy, the polygeneration system could benefit from the oxygen and hydrogen produced by renewable-powered electrolysis, which could increase the biomethane production, this will be explored in our future work. It is also worth noting that a large amount of heat is produced in the polygeneration process, which could also be considered for district heating.

The results of this process modeling work will be utilized to optimize and guide the construction of a pilot scale reactor at Mälardalen University, Västerås, Sweden. Furthermore, a concurrent investigation into economic analysis is currently underway to explore the economic feasibility of such systems.

## Acknowledgment

This work was carried out in IFAISTOS project (Intelligent electroFuel production for An Integrated STOrage System), which is funded under the framework of the joint programming initiative ERA-Net Smart Energy Systems. The initiative has received funding from the European Union's Horizon 2020 research and innovation programme under grant agreements no. 646039 and no. 755970.

## References

- [1] Van Dyk, S., Su, J., Mcmillan, J. D., & Saddler, J. (2019). Potential synergies of drop-in biofuel production with further co-processing at oil refineries. *Biofuels, Bioproducts and Biorefining*, 13(3), 760-775.
- [2] Kohl, T., Laukkanen, T. P., & Järvinen, M. P. (2014). Integration of biomass fast pyrolysis and precedent feedstock steam drying with a municipal combined heat and power plant. *Biomass and Bioenergy*, 71, 413-430.
- [3] Karvonen, J., Kunttu, J., Suominen, T., Kangas, J., Leskinen, P., & Judl, J. (2018). Integrating fast



pyrolysis reactor with combined heat and power plant improves environmental and energy efficiency in bio-oil production. *Journal of Cleaner Production*, 183, 143-152.

[4] Kohl, T., Teles, M., Melin, K., Laukkanen, T., Järvinen, M., Park, S. W., & Guidici, R. (2015). Exergoeconomic assessment of CHP-integrated biomass upgrading. *Applied energy*, 156, 290-305.

[5] Onarheim, K., Lehto, J., & Solantausta, Y. (2015). Technoeconomic assessment of a fast pyrolysis bio-oil production process integrated to a fluidized bed boiler. *Energy & Fuels*, 29(9), 5885-5893.

[6] Zetterholm, J., Wetterlund, E., Pettersson, K., & Lundgren, J. (2018). Evaluation of value chain configurations for fast pyrolysis of lignocellulosic biomass-Integration, feedstock, and product choice. *Energy*, 144, 564-575.

[7] S. Piazzi, L. Menin, D. Antolini, F. Patuzzi, and M. Baratieri, Piazzi, S., Menin, L., Antolini, D., Patuzzi, F., & Baratieri, M. (2021). Potential to retrofit existing small-scale gasifiers through steam gasification of biomass residues for hydrogen and biofuels production. *International Journal of Hydrogen Energy*, 46(13), 8972-8985.

[8] Gustavsson, C., & Hulteberg, C. (2016). Co-production of gasification based biofuels in existing combined heat and power plants—Analysis of production capacity and integration potential. *Energy*, 111, 830-840.

[9] Naqvi, M., Dahlquist, E., & Yan, J. (2017). Complementing existing CHP plants using biomass for production of hydrogen and burning the residual gas in a CHP boiler. *Biofuels*, 8(6), 675-683.

[10] Thunman, H., Gustavsson, C., Larsson, A., Gunnarsson, I., & Tengberg, F. (2019). Economic assessment of advanced biofuel production via gasification using cost data from the GoBiGas plant. *Energy Science & Engineering*, 7(1), 217-229.

[11] Holmgren, K. M., Berntsson, T. S., Andersson, E., & Rydberg, T. (2016). Comparison of integration options for gasification-based biofuel production systems—Economic and greenhouse gas emission implications. *Energy*, 111, 272-294.

[12] Salman, C. A., Naqvi, M., Thorin, E., & Yan, J. (2018). Gasification process integration with existing combined heat and power plants for polygeneration of dimethyl ether or methanol: A detailed profitability analysis. *Applied Energy*, 226, 116-128.

[13] Lisa, K., French, R. J., Orton, K. A., Dutta, A., & Schaidle, J. A. (2017). Production of low-oxygen bio-oil via ex situ catalytic fast pyrolysis and hydrotreating. *Fuel*, 207, 413-422.

[14] Dutta, A., Sahir, A., & Tan, E., (2015). Thermochemical Research Pathways with In Situ

and Ex Situ Upgrading of Fast Pyrolysis Vapors, U.S. National Renewable Energy Laboratory, NREL/TP-5100 -62455.



## Appendix

Table 3, Biooil composition

Biooil composition	Mass fraction, %	LHV, MJ/kg
Benzene	32.1	36.3
Ethanol	25.2	
Methylcyclohexane	11.6	
Cyclohexane	20.0	
Tetrahydrofurfuryl alcohol	9.7	
Ethylbenzene	1.4	

Table 4, Specifications used for reformer, water gas shift reactor, and methanation reactor

Block name	Specifications	
Gasifier (RGibbs)	Pressure	2.02 bar
	Temperature	750 - 1000 °C
	Calculation option	Calculate phase equilibrium and chemical equilibrium
Steam reformer (RGibbs)	Pressure	-0.20 bar
	Temperature	800 °C
	Calculation option	Calculate phase equilibrium and chemical equilibrium
HT-WGS (REquil)	Pressure drop	-0.35 bar
	Inlet temperature	340 °C
	Reactions	$\text{CO} + \text{H}_2\text{O} = \text{CO}_2 + \text{H}_2$
LT-WGS (REquil)	Pressure drop	-0.35 bar
	Inlet temperature	220 °C
	Reactions	$\text{CO} + \text{H}_2\text{O} = \text{CO}_2 + \text{H}_2$
Methanation reactor (REquil)	Pressure	30 bar
	Temperature	360 °C
	Reactions	$\text{CO} + \text{H}_2 = \text{CH}_4 + \text{H}_2\text{O}$
		$\text{CO}_2 + 4 \text{H}_2 = \text{CH}_4 + 2\text{H}_2\text{O}$
		$\text{CO} + \text{H}_2\text{O} = \text{CO}_2 + \text{H}_2$

Table 5, Reactions and Operating parameters in the hydrotreatment reactor

Operating parameters of the Hydrotreatment reactor		
Temperature	400 °C	
Pressure	105 bar	
Chemical reaction considered in the Hydrotreatment reactor		
Reaction number	Fractional conversion component and rate	Reactions
1	Acetic Acid, 1	$\text{Acetic Acid} + 2 \text{H}_2 = \text{Ethanol} + \text{H}_2\text{O}$
2	Furfural, 1	$\text{Furfural} + 3 \text{H}_2 = \text{Tetrahydrofurfuryl alcohol}$
3	Levogluosan, 1	$\text{Levogluosan} + \text{H}_2 + \text{H}_2\text{O} = \text{Sorbitol}$
4	M-Cresol, 0.26	$\text{H}_2 + \text{M-Cresol} = \text{Toluene} + \text{H}_2\text{O}$

5	M-Cresol, 1	$4 \text{ H}_2 + \text{M-Cresol} = \text{Methylcyclohexane} + \text{H}_2\text{O}$
6	Guaiacol, 0.2	$\text{Guaiacol} + 6 \text{ H}_2 = \text{Cyclohexane} + 2 \text{ H}_2\text{O} + \text{CH}_4$
7	Guaiacol, 1	$\text{Guaiacol} + 3 \text{ H}_2 = 2 \text{ H}_2\text{O} + \text{CH}_4 + \text{Benzene}$
8	Benzene, 0.2	$\text{Benzene} + 3 \text{ H}_2 = \text{Cyclohexane}$
9	Coniferyl Aldehyde, 0.5	$\text{Coniferyl Aldehyde} + 2 \text{ H}_2 = \text{Toluene} + 2 \text{ CO} + \text{CH}_4 + \text{H}_2\text{O}$
10	Toluene, 1	$\text{Toluene} + 3 \text{ H}_2 = \text{Methylcyclohexane}$
11	Coniferyl Aldehyde, 1	$\text{Coniferyl Aldehyde} + 3 \text{ H}_2 = \text{Ethylbenzene} + \text{CO}_2 + \text{CH}_4 + \text{H}_2\text{O}$

---